Mode-Conversion Filters

By E. A. MARCATILI

(Manuscript received July 11, 1960)

Resonance of higher-order modes in waveguides can be advantageously used to make band-rejection filters of unusually low loss and simplicity. The region where the resonance takes place can be obtained either by a local change of cross section of the waveguide or by the inclusion of dielectrics. Mode-conversion band-rejection filters can be combined to build channel-dropping filters which are of particular interest in the millimeter wavelength region to separate bands of TE_{01}° into $TE_{10}^{\square}$.

In this paper the necessary design relationships for channel-dropping filters using mode-conversion band-rejection filters are derived. It also contains a theoretical derivation of the intrinsic Q of band-rejection filters in round and rectangular waveguides. Finally, the experimental results obtained with different mode-conversion band-rejection filters at 12 and 56 kmc, and with a channel-dropping filter from TE_{01}° to $TE_{10}^{\square}$ at 56 kmc, are given.

I. INTRODUCTION

A large variety of channel-dropping filters operate through the use of band-rejection filters, and since the microwave art is pushing the usable spectrum to higher and higher frequencies, low heat loss and easy-to-build band-rejection filters are important.

This statement is particularly true in the process of separating bands in the long distance waveguide communication system[1] that operates with circular-electric mode in the millimeter wavelength region. The information sent from repeater to repeater through the low-heat-loss multimode circular waveguide must be separated into tens of bands for the purposes of regeneration and amplification at each repeater. Since each repeater operates in single-mode rectangular waveguide, one possible solution is to convert the circular-electric wave to fundamental mode in rectangular waveguide and then to drop the different channels with known techniques. This solution has several disadvantages: the filters are relatively lossy because of the low intrinsic Q of parallelepi-

ped-shaped cavities in the millimeter region, and they are difficult to build. Furthermore, the channels to be dropped last are substantially attenuated because they must travel in a high-loss rectangular waveguide. For instance, the theoretical attenuation in the standard silver waveguide RG98U (50 to 75 kmc) is 0.53 to 0.39 db/foot.

Better solutions are filters that simultaneously drop the channels and make the transfer from circular-electric wave in round waveguide to dominant mode in rectangular waveguide.[2,3]

This paper describes a channel-dropping filter that combines all the desirable features: it filters, it transfers TE_{01}° mode into $TE_{10}^{\square}$, it has low insertion loss and it is extremely easy to build. All this is possible because of the use of mode-conversion band-rejection filters.

II. DESCRIPTION OF THE MODE-CONVERSION BAND-REJECTION FILTER

Consider, for instance, a round waveguide carrying the TE_{01}° mode and barely cut off for the TE_{02}°. If for a length l the diameter of the waveguide is slightly larger, in such a way that TE_{02}° is no longer cut off, the region l becomes a multimode region[4] where the TE_{02}° generated at both diameter discontinuities can resonate and introduce a large insertion loss to the incident TE_{01}°. The bandwidth depends essentially on the amount of mode conversion (size of the discontinuity), and the center frequency depends on the length l. The filter can be made of sliding coaxial tubes because the circumferential cracks do not interrupt the conduction current of circular electric modes.

The intrinsic Q is very high, one order of magnitude better than a $TE_{101}^{\square}$ cavity, because: (a) the resonant mode is essentially a low-loss one,[1] (b) the end walls do not absorb energy since they do not exist,* (c) the tuning mechanism is lossless and (d) the coupling that is provided by the diameter change does not create high-density currents, such as exist in the case of band-rejection cavities coupled through irises to the main waveguide, or in the case of microwave band-rejection filters made of lumped elements.

The reasoning used for circular-electric modes can be generalized, that is, any waveguide that contains a low-loss, multimode region exhibits rejection bands corresponding to the resonances of the confined modes.[4,5,6,7] Thus, a rectangular waveguide cut off for $TE_{20}^{\square}$, except for a length l of slightly larger width capable of generating and supporting $TE_{20}^{\square}$, becomes a mode-conversion band-rejection filter.

* The heat loss due to the penetration of the TE_{02}° mode in the cutoff waveguides is calculated in Section IX.

Another band-rejection filter in rectangular waveguide is obtained by building the multimode region with a dielectric slab close to one of the narrow walls, since the dielectric provides an apparent width increase of the waveguide.

All these mode-conversion band-rejection filters have small return loss out of resonance.

III. DESCRIPTION OF THE CHANNEL-DROPPING FILTER

The channel-dropping filter consists of a through waveguide with two multimode regions, one of which is coupled to another waveguide (Fig. 1). For the purpose of fixing ideas, we imagine that the through waveguide is circular with two enlarged regions where the $TE_{02}°$ excited by the incident $TE_{01}°$ can resonate; the dropping arm is a rectangular waveguide. The enlarged regions where the $TE_{02}°$ mode can resonate will be referred to as *cavities*, even if they are not enclosed volumes. The idealized filter must be such that the incident $TE_{01}°$ mode is matched at all frequencies, and at midband all the power flows into the rectangular waveguide.

A low-frequency channel-dropping filter that will be demonstrated to be the equivalent of the microwave one and that satisfies the previous demands is shown in Fig. 2. The resonant circuits are equivalent to the cavities, and the three resistances connected to the circuit through ade-

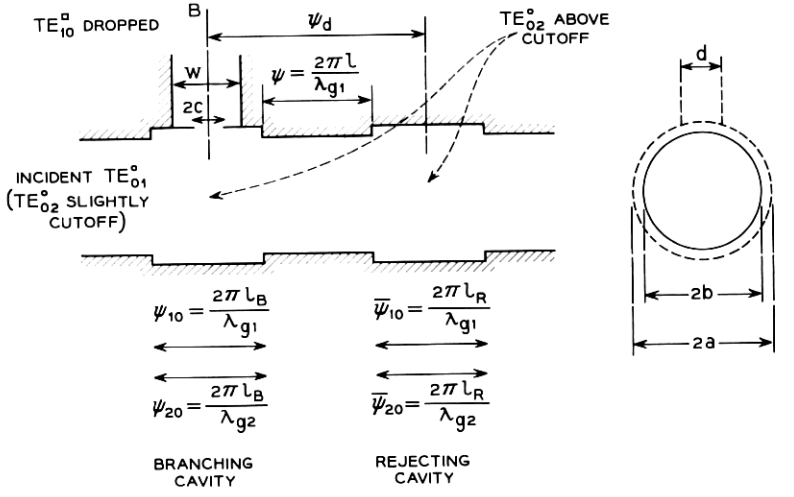

Fig. 1 — Microwave mode-conversion channel-dropping filter.

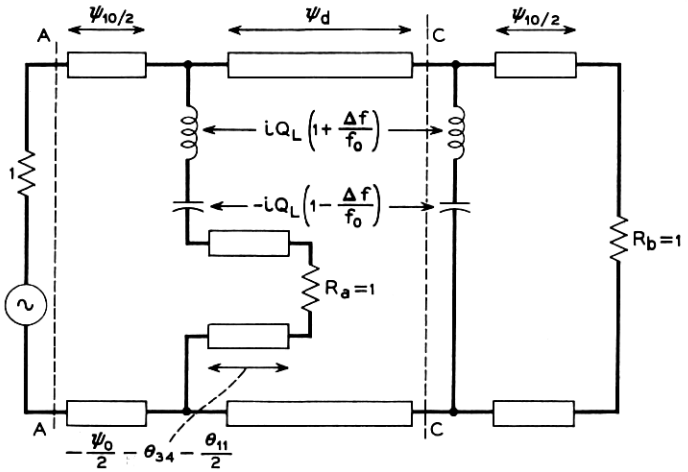

Fig. 2 — Low-frequency channel-dropping filter.

quate transformers (not indicated in the figure for simplicity) are equivalent to the characteristic impedances of the three microwave ports.

In each resonant circuit f_0 is the midband frequency and the loaded Q is defined $Q_L = f_0/(2\Delta f_0)$, where $2\Delta f_0$ is the half power bandwidth of the dropped channel. The normalized reactances are such that the impedance seen toward the right of the plane AA is unity at all frequencies, provided that ψ_d is an odd number of quarter wavelengths. At midband frequency the maximum power available goes to R_a and far from resonance it goes to R_b.

Another microwave circuit equivalent to that of Fig. 1, which may help the reader to understand the behavior of the mode-conversion channel-dropping filter, is shown in Fig. 3. Here, the resonant cavities

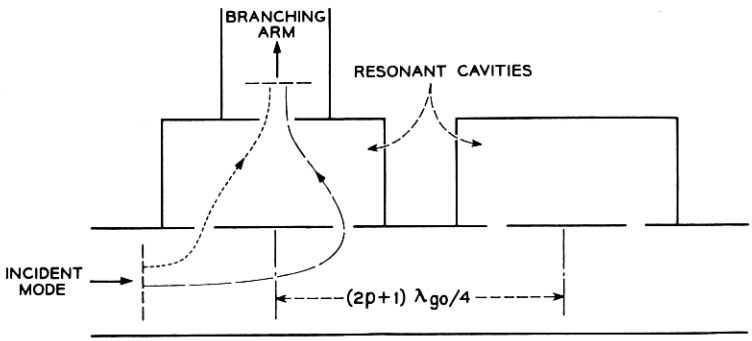

Fig. 3 — Microwave channel-dropping filter; path difference = θ_0.

have been separated from the through waveguide. The incident mode excites each cavity through two coupling holes; in an equivalent way, in Fig. 1, the incident $TE_{01}°$ mode couples to the $TE_{02}°$ of each cavity through two diameter discontinuities. Finally, in Fig. 3, only the resonant mode of the first cavity is assumed to couple to the output load, implying that the coupling between the incident and the branching mode in Fig. 1 is negligible.

The reader who is not interested in the mathematical treatment of the mode-conversion channel-dropping filter may now go directly to the résumé of results in Section VII of this paper. The scattering matrix of the branching cavity, Fig. 1, is studied in Section IV. In Section V, the scattering matrix of the rejecting cavity is derived from that of the branching cavity by reducing to zero the coupling between the round and rectangular waveguides. Then, in Section VI, both cavities are connected through a certain length of single-mode waveguide, and the mathematical description of the channel-dropping filter is completed.

The derivations have been made for single-resonance rejecting and branching filters because these are the building blocks for the design of more complicated filters such as those of the maximally flat type.[8]

IV. SCATTERING MATRIX OF THE BRANCHING CAVITY

Consider the branching cavity of Fig. 1, separated from the rejecting cavity and with all terminals matched. This cavity is represented in Fig. 4 with the elementary components separated. The symbol J_1 represents the junction where port 1′ carrying $TE_{10}□$ mode couples symmetrically to $TE_{01}°$ and $TE_{02}°$ in the cavity. Since the $TE_{02}°$ mode is almost at cut-off and close to resonance, the coupling to $TE_{01}°$ can be neglected.

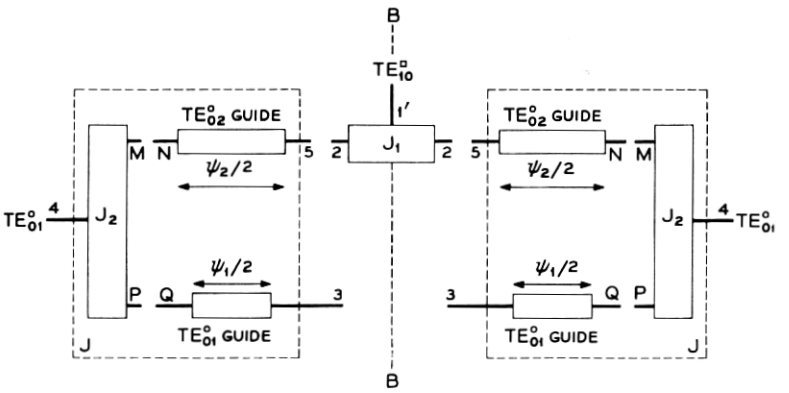

Fig. 4 — Branching cavity with elementary components separated.

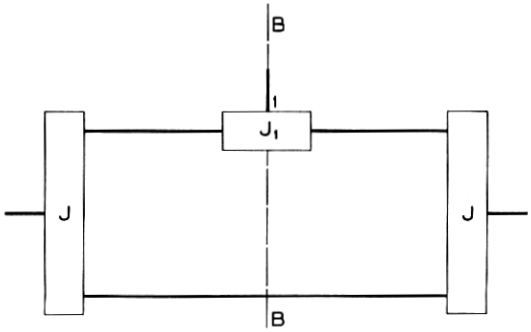

Fig. 5 — Branching cavity.

The symbol J_2 represents the junction at a diameter discontinuity; ports 4 and P carry $TE_{01}°$ and port M carries TE_{02}. Ports M and 2 are connected by a piece of waveguide whose ports are N and 5. This waveguide has a midband electrical length

$$\frac{\psi_{20}}{2} = \frac{\pi l_B}{\lambda_{g2}},$$

where l_B is the distance between diameter discontinuities and λ_{g2} is the midband $TE_{02}°$ mode guided wavelength. Likewise, ports P are connected by two pieces of waveguide, each of midband electrical length

$$\frac{\psi_{10}}{2} = \frac{\pi l_B}{\lambda_{g1}},$$

where λ_{g1} is the midband $TE_{01}°$ mode guided wavelength in the cavity.

Fig. 4 can be simplified by representing all the elements inside of each of the dotted lines as a single junction J, and so the branching cavity is reduced to the circuit shown in Fig. 5.

Since this three-port structure is symmetric with respect to the plane BB, the scattering matrix can be derived from the scattering matrices of two simpler structures, one derived by making the symmetry plane BB a magnetic plane (open circuit), that is, a surface where the tangential magnetic field is zero, and another obtained by making the symmetry plane an electric one (short circuit), that is, a surface where the electric tangential field is zero.

4.1 *Open-Circuited Half of Branching Cavity*

Assume in Fig. 5 that BB is a magnetic plane. Port 1′ as well as the branching cavity is divided in two symmetrical portions, and each half is shown in Fig. 6.

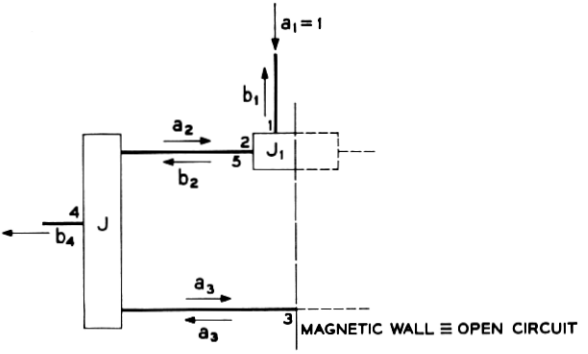

Fig. 6 — Open-circuited half of branching cavity.

If $a_1 = 1$ is the only wave incident in the structure, the outgoing waves from the junctions J and J_1 are

$$b_1 = \Gamma_{11} + a_2\Gamma_{12}, \tag{1}$$

$$b_2 = \Gamma_{12} + a_2\Gamma_{22}, \tag{2}$$

$$a_2 = b_2\Gamma_{55} + a_3\Gamma_{35}, \tag{3}$$

$$b_4 = b_2\Gamma_{45} + a_3\Gamma_{34}, \tag{4}$$

$$a_3 = a_3\Gamma_{33} + b_2\Gamma_{35}, \tag{5}$$

where Γ_{mn} represents the scattering coefficient between ports m and n.

From these five equations the scattered waves

$$b_1 = \Gamma_{11}\frac{\left(1 - \Gamma_{22}\Gamma_{55} + \frac{\Gamma_{12}^2\Gamma_{55}}{\Gamma_{11}}\right)(1 - \Gamma_{33}) - \Gamma_{22}\Gamma_{35}^2 + \frac{\Gamma_{12}^2\Gamma_{35}^2}{\Gamma_{11}}}{(1 - \Gamma_{22}\Gamma_{55})(1 - \Gamma_{33}) - \Gamma_{22}\Gamma_{35}^2} \tag{6}$$

and

$$b_4 = \Gamma_{12}\Gamma_{45}\frac{1 - \Gamma_{33} + \frac{\Gamma_{35}\Gamma_{34}}{\Gamma_{45}}}{(1 - \Gamma_{22}\Gamma_{55})(1 - \Gamma_{33}) - \Gamma_{22}\Gamma_{35}^2} \tag{7}$$

are derived. These expressions can be simplified by assuming

$$\begin{matrix} |\,\Gamma_{33}\,| \\ |\,\Gamma_{44}\,| \end{matrix} \ll \begin{matrix} |\,\Gamma_{12}\,| \\ |\,\Gamma_{35}\,| \\ |\,\Gamma_{45}\,| \end{matrix} \tag{8}$$

and

$$\left.\begin{array}{l} |\,\Gamma_{12}\,| \\ |\,\Gamma_{35}\,| \\ |\,\Gamma_{45}\,| \end{array}\right\} \ll 1. \tag{9}$$

The first assumption means that the TE_{01}° mode incident on the diameter discontinuity has negligible reflection in the same mode. This is a familiar approximation in multimode waveguide calculations, and it will also be seen later that these reflections are indeed negligible. The second assumption implies that the resonating mode TE_{02}° is loosely coupled to the other modes TE_{01}° and $TE_{10}^{\square}$.

Substituting (8) and (9) in the conservation of energy relations[9] applicable to junctions J and J_1 of Fig. 6, and neglecting terms of higher order than two, one obtains the following results:

$$\Gamma_{22}\Gamma_{55} = e^{i\varphi}(1 - |\,\Gamma_{35}\,|^2 - \tfrac{1}{2}\,|\,\Gamma_{12}\,|^2), \tag{10}$$

$$\Gamma_{22}\Gamma_{35}^{\ 2} = -|\,\Gamma_{35}\,|^2 e^{i(\theta+\varphi)}, \tag{11}$$

$$\frac{\Gamma_{12}^{\ 2}\Gamma_{55}}{\Gamma_{11}} = -|\,\Gamma_{12}\,|^2 e^{i\varphi}, \tag{12}$$

$$\frac{\Gamma_{35}\Gamma_{34}}{\Gamma_{45}} = e^{i\theta}, \tag{13}$$

in which

$$\theta = -\psi_1 + \theta_{35} - \theta_{45} + \theta_{34} \tag{14}$$

and

$$\varphi = -\psi_2 + \theta_{22} + \theta_{55}\,, \tag{15}$$

where ψ_1 and ψ_2 are the electrical distances between the branching cavity discontinuities in terms of the nonresonating and resonating modes, respectively, and θ_{mn} is the phase of the scattering coefficient between ports m and n when the waveguides are reduced to zero length.

The physical meaning of θ and φ will be given later.

Substituting (8), (10), (11), (12) and (13) in (6) and (7), leads to the simplified scattered waves

$$b_1 = \Gamma_{11}\frac{1 - \left[1 - |\,\Gamma_{35}\,|^2(1 + e^{i\theta}) + \dfrac{|\,\Gamma_{12}\,|^2}{2}\right]e^{i\varphi}}{1 - \left[1 - |\,\Gamma_{35}\,|^2(1 + e^{i\theta}) - \dfrac{|\,\Gamma_{12}\,|^2}{2}\right]e^{i\varphi}} \tag{16}$$

and

$$b_4 = \Gamma_{12}\Gamma_{45} \frac{1 + e^{i\theta}}{1 - \left[1 - |\Gamma_{35}|^2(1 + e^{i\theta}) - \frac{|\Gamma_{12}|^2}{2}\right] e^{i\varphi}}. \quad (17)$$

The values of θ and φ given in (14) and (15) are frequency-sensitive, so we define

$$\theta = \theta_0 + \Delta\theta \quad (18)$$

and

$$\varphi = \varphi_0 + \Delta\varphi, \quad (19)$$

where θ_0 and φ_0 are the values taken by θ and φ at midband frequency f_0, and $\Delta\theta$ and $\Delta\varphi$ are their small departures when the frequency is

$$f = f_0 + \Delta f \quad (20)$$

and

$$\frac{\Delta f}{f_0} \ll 1. \quad (21)$$

In this paper we choose to have the branching cavity resonating with an odd number of half wavelengths. In order to have the branching cavity resonating with an even number of half wavelengths it would be necessary to make resonant the short-circuited half of the branching cavity.

Resonance of the branching cavity (minimization of the reflected wave b_1) occurs at midband $f = f_0$ when the following relation is satisfied:

$$\varphi_0 = |\Gamma_{35}|^2 \sin\theta_0 - 2\pi s, \quad (22)$$

in which s is an integer.

If one substitutes (18), (19) and (22) in (16) and (17), and again neglects higher-order terms, the scattered waves of the branching cavity become

$$b_1 = e^{i\theta_{11}} \frac{-i\Delta\varphi + |\Gamma_{35}|^2(1 + \cos\theta_0) - \frac{|\Gamma_{12}|^2}{2}}{-i\Delta\varphi + |\Gamma_{35}|^2(1 + \cos\theta_0) + \frac{|\Gamma_{12}|^2}{2}}, \quad (23)$$

$$b_4 = \Gamma_{12}\Gamma_{45} \frac{1 + e^{i\theta_0}}{-i\Delta\varphi + |\Gamma_{35}|^2(1 + \cos\theta_0) + \frac{|\Gamma_{12}|^2}{2}}. \quad (24)$$

Several important results are deduced from the last three equations:

(a) The resonance condition, (22), as well as the scattered waves, (23) and (24), depend on the angle θ_0, which, according to (14) and (18), is the midband electrical length difference between the two possible paths that the waves may follow. These two paths are shown in both Figs. 3 and 7. The last figure is a reproduction of the branching cavity from Fig. 1, and the two paths, as well as the modes with which they are measured, have been indicated in it. If θ_0 is an odd multiple of π, the two waves cancel each other and there is no transmission through the cavity in spite of its resonance.

(b) The transmitted and reflected waves, (23) and (24), depend on $\Delta\varphi$, which is the change with frequency of the electrical length ψ_2 of the distance between diameter changes measured in the resonant mode $TE_{02}°$. But the same scattered waves are independent of $\Delta\theta$, which is the change with frequency of the electrical length θ_0.

Now it is possible to express the scattering coefficients of the open-circuited half branching cavity matrix,

$$\begin{vmatrix} S_{11} & S_{14} \\ S_{14} & S_{44} \end{vmatrix}, \tag{25}$$

in terms of b_1 and b_4.

From the definition of scattering coefficients it follows that

$$S_{11} = b_1, \tag{26}$$

$$S_{14} = b_4 \tag{27}$$

and from the conservation of energy relations[9] that

$$S_{11}{}^*S_{14} + S_{14}{}^*S_{44} = 0, \tag{28}$$

where S^* is the complex conjugate of S.

From (26), (27) and (28)

$$S_{44} = -b_1{}^*e^{i2\theta_{14}-i\psi_2}. \tag{29}$$

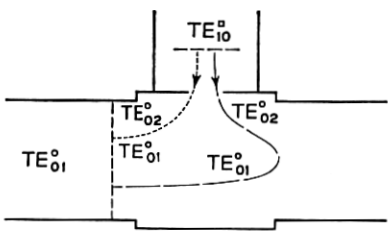

Fig. 7 — Branching cavity; path difference = θ_0.

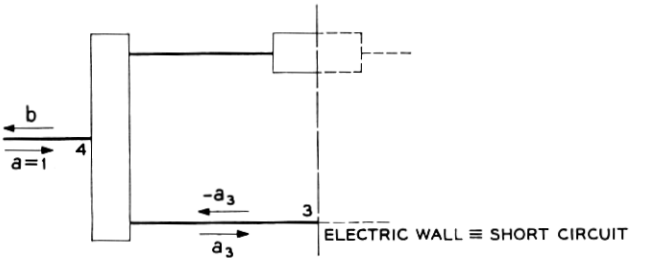

Fig. 8 — Short-circuited half of branching cavity.

4.2 *Short-Circuited Half of Branching Cavity*

Consider again the branching cavity equivalent circuit in Fig. 5, and let BB represent a perfectly conducting surface. One of the halves of the bisected circuit is shown in Fig. 8. A unitary wave fed in port 4 yields, because of the absence of resonance

$$b \cong -e^{-i\psi_1+2i\theta_{34}}. \tag{30}$$

The scattering matrix is $S = b$.

4.3 *Scattering Matrix of the Branching Cavity*

Fig. 9 represents the branching cavity. Considering symmetry and reciprocity, the scattering matrix is

$$\begin{vmatrix} S_{66} & S_{67} & S_{68} \\ S_{67} & S_{77} & S_{67} \\ S_{68} & S_{67} & S_{66} \end{vmatrix}. \tag{31}$$

All the scattering coefficients in (31) are determined as follows:

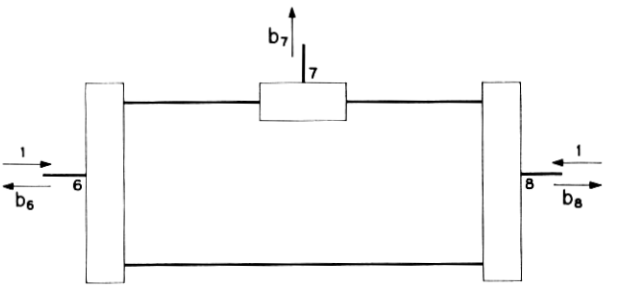

Fig. 9 — Branching cavity with waves fed in phase.

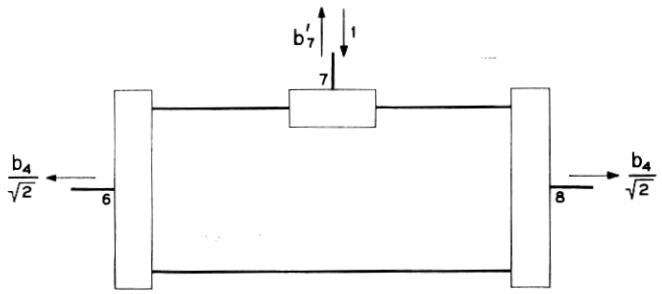

Fig. 10 — Branching cavity with signal fed in branching arm.

Feed unit power into ports 6 and 8 such that the phases of the electric fields are the same. The plane of symmetry becomes a magnetic plane, and the scattered waves derived from (26), (27), (29) and (30) are

$$b_6 = S_{66} + S_{68} = -b_1^* e^{i2\theta_{14} - i\psi_2}, \tag{32}$$

$$b_7 = 2S_{67} = \sqrt{2} b_4 . \tag{33}$$

If unit power is fed into port 7, of Fig. 10, the reflection is

$$b_7' = S_{77} = b_1 . \tag{34}$$

Finally, if port 6 and 8 of Fig. 11 are fed 180° out of phase with unit power, the plane of symmetry which has zero tangential electric field becomes a short circuit, and the scattered wave is obtained from (30):

$$b_6' = S_{66} - S_{68} = -e^{-i\psi_1 + i2\theta_{34}}. \tag{35}$$

Substituting the explicit values of b_1 and b_4 given in (23) and (24), in (32), (33), (34) and (35), and, solving this set of equations for the

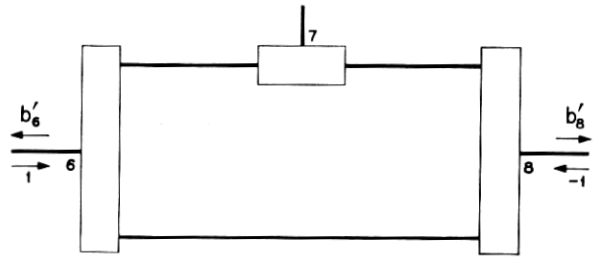

Fig. 11 — Branching cavity with waves fed in opposite phase.

scattering coefficients of the branching cavity, one obtains

$$S_{66} = -e^{i(2\theta_{34}-\psi_1)} \frac{|\Gamma_{35}|^2(1+\cos\theta_0)}{-i\Delta\varphi + \frac{|\Gamma_{12}|^2}{2} + |\Gamma_{35}|^2(1+\cos\theta_0)}, \tag{36}$$

$$S_{67} = e^{i(\varphi/2+\theta_{34}-\psi_1/2+\theta_{11}/2)} \frac{|\Gamma_{12}||\Gamma_{35}|(1+\cos\theta_0)^{\frac{1}{2}}}{-i\Delta\varphi + \frac{|\Gamma_{12}|^2}{2} + |\Gamma_{35}|^2(1+\cos\theta_0)}, \tag{37}$$

$$S_{68} = e^{i(2\theta_{34}-\psi_1)} \frac{-i\Delta\varphi + \frac{|\Gamma_{12}|^2}{2}}{-i\Delta\varphi + \frac{|\Gamma_{12}|^2}{2} + |\Gamma_{35}|^2(1+\cos\theta_0)}, \tag{38}$$

$$S_{77} = e^{i\theta_{11}} \frac{-i\Delta\varphi - \frac{|\Gamma_{12}|^2}{2} + |\Gamma_{35}|^2(1+\cos\theta_0)}{-i\Delta\varphi + \frac{|\Gamma_{12}|^2}{2} + |\Gamma_{35}|^2(1+\cos\theta_0)}. \tag{39}$$

V. SCATTERING MATRIX OF THE REJECTING CAVITY

The elements of the scattering matrix of the rejecting cavity

$$\begin{vmatrix} \bar{S}_{66} & \bar{S}_{68} \\ \bar{S}_{68} & \bar{S}_{66} \end{vmatrix} \tag{40}$$

can be deduced from those of the branching cavity (36) and (38) by eliminating the coupling to the rectangular waveguide, that is, making

$$\Gamma_{12} = 0. \tag{41}$$

The dash over the characters is to distinguish them from those of the branching cavity:

$$\bar{S}_{66} = -e^{i(2\bar{\theta}_{34}-\bar{\psi}_1)} \frac{1}{1 - \frac{i\Delta\bar{\varphi}}{|\bar{\Gamma}_{35}|^2(1+\cos\bar{\theta}_0)}} \tag{42}$$

$$\bar{S}_{68} = e^{i(2\bar{\theta}_{34}-\psi_1)} \frac{\frac{i\Delta\bar{\varphi}}{|\bar{\Gamma}_{35}|^2(1+\cos\bar{\theta}_0)}}{1 - \frac{i\Delta\bar{\varphi}}{(\bar{\Gamma}_{35})^2(1+\cos\bar{\theta}_0)}}. \tag{43}$$

At midband, $\Delta\bar{\varphi} = 0$ and

$$\bar{S}_{66} = -e^{i(2\theta_{34}-\psi_1)}. \tag{44}$$

This means that at resonance the cavity acts as a short circuit located at half the length of the cavity. Again, as in the case of the branching cavity, if

$$\bar{\theta}_0 = (2n + 1)\pi \tag{45}$$

there is no resonance.

VI. SCATTERING COEFFICIENTS OF THE CHANNEL-DROPPING FILTER

Knowing the scattering matrices of the branching and rejecting cavities, we will find the scattering elements of the circuit obtained by joining a branching cavity and a rejecting cavity with a piece of waveguide of electrical length ψ. From the block diagram representation of the branching filter in Fig. 12,

$$B_1 = S_{66} + AS_{68}\,, \tag{46}$$

$$B_2 = S_{67}(1 + A), \tag{47}$$

$$B_3 = Be^{-i\psi}\bar{S}_{68}\,, \tag{48}$$

$$B = S_{68} + AS_{66}\,, \tag{49}$$

$$A = B\bar{S}_{66}e^{-i2\psi}. \tag{50}$$

First it will be demonstrated that, if certain conditions are satisfied, port 1 of the filter (Fig. 12) is matched at all frequencies; then the values of B_2 and B_3 will be ascertained.

From (46), (49) and (50)

$$B_1 = S_{66}\frac{1 - \left(S_{66}\bar{S}_{66} - \dfrac{\bar{S}_{66}}{\bar{S}_{66}}S_{68}^{\,2}\right)e^{-i2\psi}}{1 - S_{66}\bar{S}_{66}e^{-i2\psi}}. \tag{51}$$

Replacing S_{66}, S_{68} and $\bar{S}_{66}$ in the numerator with the values given in (36), (38) and (42), one obtains

$$B_1 = S_{66}\frac{1 - e^{i2(\theta_{34}+\theta_{34}-\psi-\psi_1/2-\bar{\psi}_1/2)}\dfrac{1 - \dfrac{|\Gamma_{12}|^2}{2} - i\Delta\varphi}{|\Gamma_{35}|^2(1 + \cos\theta_0)}}{1 - \dfrac{i\Delta\bar{\varphi}}{|\bar{\Gamma}_{35}|^2(1 + \cos\bar{\theta}_0)}}}{1 - S_{66}\bar{S}_{66}e^{-i2\psi}}. \tag{52}$$

In order to have port 1 of the channel-dropping filter matched at all

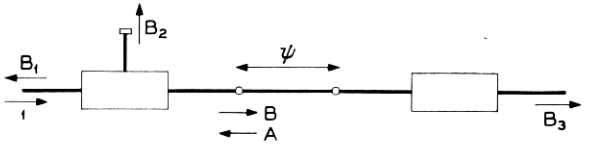

Fig. 12 — Block diagram of the channel-dropping filter.

frequencies, the reflected wave B_1 must vanish. The conditions to be satisfied are

$$\bar{\Gamma}_{35} = \Gamma_{35}, \tag{53}$$

$$\bar{\theta}_0 = \theta_0, \tag{54}$$

$$\bar{\theta}_{34} = \theta_{34}, \tag{55}$$

$$\Delta\bar{\varphi} = \Delta\varphi, \tag{56}$$

$$\theta_{34} + \bar{\theta}_{34} - \psi - \frac{\psi_1}{2} - \frac{\bar{\psi}_1}{2} = -\frac{\pi}{2}(1 + 2p), \tag{57}$$

where p is an arbitrary integer, and

$$|\Gamma_{12}|^2 = 4\,|\Gamma_{35}|^2(1 + \cos\theta_0). \tag{58}$$

Conditions (53), (54), (55) and (56) state that, except for a small-length correction due to the effect of the coupling to the dropping waveguide, both resonating cavities must be equal. Condition (57) establishes that the distance between the centers of the resonating cavities must be an odd number of quarters of guided wavelength of the non-resonant mode. Since this condition is fulfilled rigorously only at discrete frequencies, the length of the cavities and the distance between them must be selected as short as possible. Finally, condition (58) states that in the branching cavity, Fig. 7, the power coupled from the resonating mode TE_{02}° to the dropped mode $TE_{10}^{\square}$, must be equal to four times the power coupled to each one of the TE_{01}° ports.

Substituting (53) through (58) in the expressions of the branched and through waves (47) and (48), one finds that

$$B_2 = e^{i(\varphi/2+\theta_{34}-\psi_1/2+\theta_{11}/2)}\,\frac{1}{1 - \dfrac{i\Delta\varphi}{2\,|\Gamma_{35}|^2(1+\cos\theta_0)}}, \tag{59}$$

$$B_3 = -e^{i(-\psi+4\theta_{34}-2\psi_1)}\,\frac{\dfrac{i\Delta\varphi}{2\,|\Gamma_{35}|^2(1+\cos\theta_0)}}{1 - \dfrac{i\Delta\varphi}{2\,|\Gamma_{35}|^2(1+\cos\theta_0)}}. \tag{60}$$

At resonance, $\Delta\varphi = 0$ and B_2 and B_3 become

$$B_2 = e^{i(\varphi_0/2+\theta_{34}-\psi_1/2+\theta_{11}/2)}, \tag{61}$$

$$B_3 = 0. \tag{62}$$

Far from resonance,

$$\frac{|\, i\Delta\varphi \,|}{2\,|\,\Gamma_{35}\,|^2\,(1+\cos\theta_0)} \gg 1 \tag{63}$$

and

$$B_2 = 0, \tag{64}$$

$$B_3 = e^{i(-\psi+4\theta_{34}-2\psi_1)}. \tag{65}$$

In order to introduce the concept of loaded Q or Q_L of the channel-dropping filter, the value of $\Delta\varphi$ will be expressed as a function of frequency. $\Delta\varphi$ is the difference between the electrical length of the resonating cavity at midband f_0 and at any other frequency $f_0 + \Delta f$. From (15),

$$\Delta\varphi = \Delta f \frac{d\varphi_0}{df_0} \cong -\frac{\Delta f}{f_0}\,\psi_{20}\,\frac{\lambda_{g2}^{\,2}}{\lambda_0^{\,2}} + \Delta f \frac{d}{df_0}\,(\theta_{22}+\theta_{55}) \tag{66}$$

provided that

$$\left(\frac{\lambda_0}{\lambda_{g2}}\right)^2 \gg \frac{|\, 2\Delta f \,|}{f_0}, \tag{67}$$

in which λ_0 and λ_{g2} are the free-space wavelength and guided wavelength of the resonating mode at midband f_0, and ψ_{20} is the midband electrical distance between the diameter discontinuities of the branching cavity measured in terms of the resonating $TE_{02}{}^\circ$ mode.

Substituting (66) in (59) and (60) leads to

$$B_2 = e^{i(\varphi/2+\theta_{34}-\psi_1/2+\theta_{11}/2)}\,\frac{1}{1+i2Q_L\dfrac{\Delta f}{f_0}}, \tag{68}$$

$$B_3 = e^{i(-\psi+4\theta_{34}-2\psi_1)}\,\frac{i2Q_L\dfrac{\Delta f}{f_0}}{1+i2Q_L\dfrac{\Delta f}{f_0}}, \tag{69}$$

where

$$Q_L = \frac{\psi_{20}\left(\dfrac{\lambda_{g2}}{\lambda_0}\right)^2 - f_0\dfrac{d}{df_0}\,(\theta_{22}+\theta_{55})}{4\,|\,\Gamma_{35}\,|^2\,(1+\cos\theta_0)}. \tag{70}$$

The loaded Q is, as expected, inversely proportional to the power coupled into the resonant mode, but that coupling is not enough to insure a finite Q_L. If θ_0, the electrical path difference discussed above and shown in Figs. 3 and 7, is an odd multiple of π, then Q_L becomes infinitely large. Also, as expected, at the frequency at which the resonating mode passes through cutoff, λ_{g2} becomes infinite and Q_L diverges.

It can be shown that (68) and (69) are the transfer coefficients of the low-frequency circuit in Fig. 2, and consequently this circuit is the equivalent to that in Fig. 1.

For the purpose of testing the cavities independently of each other it is important to know their scattering coefficients. They are obtained by substituting (66) and (70) in (36), (37), (38), (39), (42) and (43):

$$S_{66} = -e^{i(2\theta_{34}-\psi_1)} \frac{1}{3 + i4\dfrac{\Delta f}{f_0} Q_L}, \tag{71}$$

$$S_{67} = e^{i(\varphi/2+\theta_{34}-\psi_1/2+\theta_{11}/2)} \frac{2}{3 + i4\dfrac{\Delta f}{f_0} Q_L}, \tag{72}$$

$$S_{68} = e^{i(2\theta_{34}-\psi_1)} \frac{2 + i4\dfrac{\Delta f}{f_0} Q_L}{3 + i4\dfrac{\Delta f}{f_0} Q_L}, \tag{73}$$

$$S_{77} = e^{i\theta_{11}} \frac{-1 + i4\dfrac{\Delta f}{f_0} Q_L}{3 + i4\dfrac{\Delta f}{f_0} Q_L}, \tag{74}$$

$$\bar{S}_{66} = -e^{i(2\theta_{34}-\psi_1)} \frac{1}{1 + i4\dfrac{\Delta f}{f_0} Q_L}, \tag{75}$$

$$\bar{S}_{68} = e^{i(2\theta_{34}-\psi_1)} \frac{i4\dfrac{\Delta f}{f_0} Q_L}{1 + i4\dfrac{\Delta f}{f_0} Q_L}. \tag{76}$$

Considering first the branching cavity, from (71) to (74), it is concluded that at midband the amplitude of the reflection at any port is one-third and the amplitude of the transmission to any other port is

two-thirds. Furthermore, the half power band of the reflection characteristic, (71), is

$$\frac{3}{2}\frac{f_0}{Q_L}.$$

For the rejecting cavity, the loaded Q, (75) or (76), is twice the loaded Q of design of the channel-dropping filter.

VII. RÉSUMÉ OF FORMULAS FOR THE DIMENSIONING OF A CHANNEL-DROPPING FILTER

The information given is the midband frequency f_0 and the half power bandwidth of the dropped channel $2\Delta f_0$, defined in terms of the loaded Q:

$$Q_L = \frac{f_0}{2\Delta f_0}. \tag{77}$$

The unknowns are:

ψ_{20}, midband electrical distance between diameter discontinuities of the branching cavity measured in terms of the resonating mode,

$\bar{\psi}_{20}$, midband electrical distance between diameter discontinuities of the rejecting cavity measured in terms of the resonating mode,

ψ_d, midband electrical distance between centers of cavities in terms of the nonresonating mode,

$2\Gamma_{35}(1 + \cos\theta_0)^{\frac{1}{2}}$, coupling coefficient between the resonating mode and the through waveguide,

$\sqrt{2}\Gamma_{12}$, coupling coefficient between the resonating mode and the dropping mode.

From (15) and (22),

$$\psi_{20} = \theta_{22} + \theta_{55} - |\Gamma_{35}|^2 \sin\theta_0 + 2\pi s = \frac{2\pi l_B}{\lambda_{g2}}, \tag{78}$$

where θ_0 reproduced from (14) is

$$\theta_0 = -\psi_{10} + \theta_{34} + \theta_{35} - \theta_{45} \tag{79}$$

and ψ_{10} is the midband electrical distance between diameter discontinuities of the branching cavity measured in terms of the nonresonating mode; θ_{mn} is the phase of the scattering coefficients between ports m and n, Fig. 4, with waveguide lengths reduced to zero; l_B is the length of the branching cavity and λ_{g2} is the midband resonant mode guided wavelength.

For the rejecting cavity $\theta_{22} = 0$; then, from (78),

$$\bar{\psi}_{20} = \theta_{55} - |\Gamma_{35}|^2 \sin\bar{\theta}_0 + 2\pi s = \frac{2\pi l_R}{\lambda_{g2}}, \tag{80}$$

l_R being the length of the rejecting cavity, and

$$\bar{\theta}_0 = -\bar{\psi}_{10} + \theta_{34} + \theta_{35} - \theta_{45}. \tag{81}$$

From (57),

$$\psi_d = \psi_0 + \frac{\psi_{10}}{2} + \frac{\bar{\psi}_{10}}{2} - 2\theta_{34} = \frac{\pi}{2}(1 + 2p), \tag{82}$$

where ψ_0 is the midband electrical distance between cavities and p is an arbitrary integer. From (58) and (70),

$$|\Gamma_{35}|^2(1 + \cos\theta_0) = \frac{|\Gamma_{12}|^2}{4} = \frac{\psi_{20}\left(\frac{\lambda_{g2}}{\lambda_0}\right)^2 - f_0\frac{d}{df_0}(\theta_{22} + \theta_{55})}{4Q_L}. \tag{83}$$

From the theory of diffraction by small holes,[10]

$$\theta_{22} = \frac{4\pi c^3}{3\lambda_0}\sqrt{\frac{\mu}{\epsilon}}\frac{|H_2^2|}{P_2}, \tag{84}$$

$$|\Gamma_{12}| = \frac{2^{\frac{5}{2}}}{3}\frac{\pi c^3}{\lambda_0}\sqrt{\frac{\mu}{\epsilon}}\frac{|H_1||H_2|}{\sqrt{P_1P_2}}, \tag{85}$$

where c is the radius of the round hole that couples the resonating to the branching mode, and μ and ϵ are the permeability and permittivity of free space. If one considers that the standing resonating field is made of two waves propagating in opposite directions, $|H_2|$ is the absolute value of the magnetic field of one of those waves at the hole and P_2 is the average power carried by such a wave; $|H_1|$ is the absolute value of the magnetic field at the hole of a wave in the branching waveguide and P_1 is the average power carried by such a wave.

The values of θ_{22}, θ_{34}, θ_{55}, θ_0, $|\Gamma_{35}|$, H_1, H_2, P_1, P_2 depend on the particular structure selected for the filter.

7.1 *Channel-Dropping Filter from Mode TE_{01}° in Circular Waveguide to TE_{10}□ in Rectangular Waveguide*

In Fig. 1 let us call a and b the radii of the double- and single-mode regions respectively, and W and d the width and height of the rectangular waveguide.

From Ref. 11,

$$\theta_{55} = -2 \operatorname{arctg} \left\{ \frac{Y_{2a}}{|Y_{2b}|} \left[\frac{J_1[v_2(1-\delta)]}{\delta\left(1+\frac{\delta}{2}\right)v_2 J_0(v_2)} \right]^2 \right\} \pm \pi, \tag{86}$$

$$\theta_{35} - \theta_{45} = 2\frac{|Y_{2b}|}{Y_{1a}} \pm \pi, \tag{87}$$

$$\theta_{34} = 0 \tag{88}$$

and

$$|\Gamma_{35}|^2 \cong \frac{Y_{1a}}{Y_{2a}} \left[\frac{2\delta v_2^2}{v_2^2 - v_1^2} \frac{J_0(v_2)}{J_0(v_1)} \frac{J_1[v_1(1-\delta)]}{J_1[v_2(1-\delta)]} \right]^2 \frac{1 + \left|\frac{Y_{2b}}{Y_{1b}}\right|^2}{1 + \left|\frac{Y_{2b}}{Y_{2a}}\right|^2}, \tag{89}$$

where

$$Y_{mb} = \sqrt{\frac{\epsilon}{\mu}} \sqrt{1 - \left(\frac{v_m \lambda_0}{2\pi b}\right)^2}, \tag{90}$$

$$Y_{na} = \sqrt{\frac{\epsilon}{\mu}} \sqrt{1 - \left(\frac{v_n \lambda_0}{2\pi a}\right)^2}, \tag{91}$$

$$\delta = 1 - \frac{b}{a}. \tag{92}$$

J_n is the Bessel function of the first kind and order n, v_p is the pth root of the J_1 function.

From Ref. 12, pp. 58–59,

$$\frac{H_2^2}{P_2} = \frac{v_2^2 \sqrt{\frac{\epsilon}{\mu}}}{2\pi^3 \sqrt{1 - \left(\frac{v_2 \lambda_0}{2\pi a}\right)^2}} \frac{\lambda^2}{a^4}. \tag{93}$$

From Ref. 12, p. 55, if the round hole is at the center of the rectangular waveguide cross section,

$$\frac{|H_1|}{\sqrt{P_1}} = 2\left[\frac{\sqrt{\frac{\epsilon}{\mu}} \sqrt{1 - \left(\frac{\lambda_0}{2W}\right)^2}}{Wd} \right]^{\frac{1}{2}}. \tag{94}$$

Substituting (93) and (94) in (84) and (85) results in

$$\theta_{22} = \frac{2v_2^2}{3\pi^2\sqrt{1-\left(\frac{v_2\lambda_0}{2\pi a}\right)^2}}\frac{\lambda_0 c^3}{a^4}, \tag{95}$$

$$|\Gamma_{12}| = \frac{8v_2}{3\pi^{\frac{1}{2}}}\left[\frac{1-\left(\frac{\lambda_0}{2W}\right)^2}{1-\left(\frac{v_2\lambda_0}{2\pi a}\right)^2}\right]^{\frac{1}{2}}\frac{c^3}{(Wd)^{\frac{1}{2}}a^2}. \tag{96}$$

Expressions (78), (79), (80), (81), (82), (83), (86), (89), (95) and (96) are the general relations necessary to determine the dimensions of the filter. As an aid in their solution it is convenient to have the approximate results obtained when the expressions are drastically simplified by the following assumptions: all corrective terms due to coupling effects are neglected; the cutoff radius for $TE_{02}°$ at midband is selected at $a(1-\delta/2)$; and

$$v_2\delta \ll 1. \tag{97}$$

These approximate results are

$$\psi_{20} = \bar{\psi}_{20} = \theta_{55} + 2\pi s = \frac{2\pi l_B\sqrt{\delta}}{\lambda_0} = \frac{2\pi l_R\sqrt{\delta}}{\lambda_0}, \tag{98}$$

$$\theta_0 = \bar{\theta}_0 = -\psi_{10} \pm \pi = -\frac{2\pi l_B}{\lambda_0} \pm \pi, \tag{99}$$

$$\psi_d = \psi + \psi_{10} = \frac{\pi}{2}(1+2p), \tag{100}$$

$$|\Gamma_{35}|^2\left(1+\cos\frac{\pi}{2\sqrt{\delta}}\right) = \frac{|\Gamma_{12}|^2}{4} = \frac{\psi_{20}}{4Q_L\delta}, \tag{101}$$

$$\theta_{55} = \frac{\pi}{2}, \tag{102}$$

$$|\Gamma_{35}|^2 = 2\delta^{\frac{3}{2}}\left(\frac{v_1v_2}{v_2^2-v_1^2}\right)^2, \tag{103}$$

$$|\Gamma_{12}| = \frac{8v_2}{3\pi^{\frac{1}{2}}}\left[\frac{1-\left(\frac{\lambda_0}{2W}\right)^2}{\delta}\right]^{\frac{1}{2}}\frac{c^3}{(Wd)^{\frac{1}{2}}a^2}, \tag{104}$$

and explicitly,

$$a = \frac{v_2\lambda_0}{2\pi}\left(1 + \frac{\delta}{2}\right) = 1.117\,\lambda_0\left(1 + \frac{\delta}{2}\right), \tag{105}$$

$$b = \frac{v_2\lambda_0}{2\pi}\left(1 - \frac{\delta}{2}\right) = 1.117\,\lambda_0\left(1 - \frac{\delta}{2}\right), \tag{106}$$

$$l_B = l_R = \frac{\lambda_0}{4\sqrt{\delta}}\,(1 + 4s), \tag{107}$$

$$l = \frac{\lambda_0}{4}\left(1 + 2p - \frac{1 + 4s}{\sqrt{\delta}}\right), \tag{108}$$

$$\begin{aligned} 2c &= \lambda_0\left\{\frac{9v_2^{\,2}}{32\pi^2}\,\frac{Wd(1 + 4s)}{\lambda_0^{\,2}Q_L\delta^{\frac{1}{2}}\left[1 - \left(\frac{\lambda}{2W}\right)^2\right]^{\frac{1}{2}}}\right\}^{\frac{1}{6}} \\ &= \lambda_0\left\{1.4\,\frac{Wd(1 + 4s)}{\lambda_0^{\,2}Q_L\delta^{\frac{1}{2}}\left[1 - \left(\frac{\lambda_0}{2W}\right)^2\right]^{\frac{1}{2}}}\right\}^{\frac{1}{6}}, \end{aligned} \tag{109}$$

$$\begin{aligned} \delta\left(1 - \cos\frac{\pi}{2\sqrt{\delta}}\right)^{\frac{2}{3}} &= \left(\frac{\pi}{16}\right)^{\frac{2}{3}}\left[\frac{v_2^{\,2} - v_1^{\,2}}{v_1v_2}\right]^{\frac{4}{3}}\left(\frac{1 + 4s}{Q_L}\right)^{\frac{2}{3}} \\ &= 0.639\left(\frac{1 + 4s}{Q_L}\right)^{\frac{2}{3}}. \end{aligned} \tag{110}$$

Since Q_L and λ_0 are given, the dimensions of the filter can be obtained by calculating δ from (110) by successive approximations and substituting this value in the relations (105) through (108).

Far from resonance, the amplitude of the reflection of the $TE_{01}°$ mode at each diameter change, derived from Ref. 11, is

$$|\,\Gamma_{11}\,| = |\,\Gamma_{33}\,| = \left(\frac{v_1}{v_2}\right)^2\frac{\delta}{2} = 0.15\,\delta. \tag{111}$$

7.2 *Channel-Dropping Filter from Mode $TE_{10}^{\square}$ in Rectangular Waveguide to $TE_{10}^{\square}$ in Rectangular Waveguide*

Calling a and b the widths of the through waveguide in the double and single mode regions, respectively, W the width of the branching rectangular waveguide and d the height of all of them, one obtains from Ref. 11

$$\theta_{55} = -2\,\text{arctg}\,\frac{Y_{2a}}{|\,Y_{2b}\,|}\,\frac{(\sin 2\pi\delta)^2}{(2\pi\delta)} \pm \pi, \tag{112}$$

$$\theta_{35} - \theta_{45} = 2\frac{|Y_{2b}|}{Y_{1b}} \pm \pi, \tag{113}$$

$$\theta_{34} = 0, \tag{114}$$

$$|\Gamma_{35}|^2 = \frac{Y_{1a}}{Y_{2a}}\left(\frac{8\delta}{3}\frac{\sin \pi\delta}{\sin 2\pi\delta}\right)^2 \frac{1 + \left|\frac{Y_{2b}}{Y_{1b}}\right|^2}{1 + \left|\frac{Y_{2b}}{Y_{2a}}\right|^2}, \tag{115}$$

where

$$Y_{mb} = \sqrt{\frac{\epsilon}{\mu}}\sqrt{1 - \left(\frac{m\lambda_0}{2b}\right)^2}, \tag{116}$$

$$Y_{na} = \sqrt{\frac{\epsilon}{\mu}}\sqrt{1 - \left(\frac{n\lambda_0}{2a}\right)^2}, \tag{117}$$

$$\delta = 1 - \frac{b}{a}. \tag{118}$$

From Ref. 9, p. 55, if the round hole is at the center of the branching rectangular waveguide cross section,

$$\frac{H_2^2}{P_2} = \frac{4\sqrt{\frac{\epsilon}{\mu}}}{\sqrt{1 - \left(\frac{\lambda_0}{a}\right)^2}}\frac{\lambda_0^2}{a^3 d}, \tag{119}$$

$$\frac{H_1}{\sqrt{P_1}} = 2\left[\frac{\sqrt{\frac{\epsilon}{\mu}}\sqrt{1 - \left(\frac{\lambda_0}{2W}\right)^2}}{Wd}\right]^{\frac{1}{2}}. \tag{120}$$

Substituting (119) and (120) in (84) and (85) yields

$$\theta_{22} = \frac{16\pi}{3\sqrt{1 - \left(\frac{\lambda_0}{a}\right)^2}}\frac{\lambda_0 c^3}{a^3 d} \tag{121}$$

$$|\Gamma_{12}| = \frac{2^{\frac{3}{2}}\pi}{3}\left[\frac{1 - \left(\frac{\lambda_0}{2W}\right)^2}{1 - \left(\frac{\lambda_0}{a}\right)^2}\right]^{\frac{1}{4}}\frac{c^3}{(a^3 d^2 W)^{\frac{1}{2}}}. \tag{122}$$

Again, expressions (78), (79), (80), (81), (82), (83), (86), (89), (95) and (96) can be simplified under the following assumptions: All corrective terms due to coupling effects are neglected; the cutoff width for

$TE_{20}^{\square}$ at midband is $a(1 - \delta/2)$; and

$$2\pi\delta \ll 1. \tag{123}$$

Then

$$\psi_{20} = \bar{\psi}_{20} = \theta_{55} = \frac{2\pi l_B\sqrt{\delta}}{\lambda_0} = \frac{2\pi l_R\sqrt{\delta}}{\lambda_0}, \tag{124}$$

$$\theta_0 = -\psi_{10} \pm \pi = -\frac{\pi}{2\sqrt{\delta}} \pm \pi, \tag{125}$$

$$\psi_d = \psi + \psi_{10} = \frac{\pi}{2}(1 + 2p), \tag{126}$$

$$|\Gamma_{35}|^2\left(1 + \cos\frac{\pi}{2\sqrt{\delta}}\right) = \frac{|\Gamma_{12}|^2}{4} = \frac{|\psi_{2B}|}{4Q_L\delta}. \tag{127}$$

$$\theta_{55} = \frac{\pi}{2} + 2s\pi, \tag{128}$$

$$|\Gamma_{35}|^2 = \tfrac{8}{9}\delta^{\frac{3}{2}}, \tag{129}$$

$$|\Gamma_{12}| = \frac{2^{\frac{3}{2}}\pi}{3}\left[\frac{1 - \left(\frac{\lambda_0}{2W}\right)^2}{\delta}\right]^{-\frac{1}{4}}\frac{c^3}{(a^3W)^{\frac{1}{2}}d}, \tag{130}$$

and explicitly

$$a = \lambda_0\left(1 + \frac{\delta}{2}\right), \tag{131}$$

$$b = \lambda_0\left(1 - \frac{\delta}{2}\right), \tag{132}$$

$$l_B = l_R = \frac{\lambda_0(1 + 4s)}{4\sqrt{\delta}}, \tag{133}$$

$$l = \frac{\lambda_0}{4}\left(1 + 2p - \frac{1 + 4s}{\sqrt{\delta}}\right), \tag{134}$$

$$2c = \lambda_0\left\{\frac{9}{8\pi}\frac{Wd^2(1 + 4s)}{Q_L\delta^{\frac{1}{2}}\left[1 - \left(\frac{\lambda_0}{2W}\right)^2\right]^{\frac{1}{2}}\lambda_0^3}\right\}^{\frac{1}{6}} \tag{135}$$

$$= \lambda_0\left\{0.358\frac{Wd^2(1 + 4s)}{Q_L\delta^{\frac{1}{2}}\left[1 - \left(\frac{\lambda_0}{2W}\right)^2\right]^{\frac{1}{2}}\lambda_0^2}\right\}^{\frac{1}{6}}$$

$$\left(1 - \cos\frac{\pi}{2\sqrt{\delta}}\right)^{\frac{3}{5}} = \left[\frac{9\pi(1 + 4s)}{64Q_L}\right]^{\frac{3}{5}} = 0.72\left(\frac{1 + 4s}{Q_L}\right)^{\frac{3}{5}}. \tag{136}$$

Given Q_L and λ_0, the dimensioning of the filter is obtained by calculating δ from (136) and replacing this value in the explicit dimensions (131) through (135).

Far from resonance, the amplitude of the reflection of the $TE_{10}^{\square}$ mode at each width change, derived from Ref. 11, is

$$| \Gamma_{11} | = | \Gamma_{13} | = 0.125\delta.$$

VIII. DESIGN OF MODE-CONVERSION BAND-REJECTION FILTERS

In order to build multipole mode-conversion band-rejection filters, it is necessary to know explicitly the scattering coefficients of a single cavity. These coefficients, given in (42) and (43), can be rewritten with the help of (66) as

$$\bar{S}_{66} = -e^{i(2\theta_{34}-\bar{\psi}_1)} \frac{1}{1 + i2\bar{Q}_L \frac{\Delta f}{f_0}}, \tag{137}$$

$$\bar{S}_{68} = e^{i(2\theta_{34}-\bar{\psi}_1)} \frac{i2\bar{Q}_L \frac{\Delta f}{f_0}}{1 + i2\bar{Q}_L \frac{\Delta f}{f_0}}, \tag{138}$$

where

$$\bar{Q}_L = \frac{\bar{\psi}_{20}\left(\frac{\bar{\lambda}_{g2}}{\lambda_0}\right)^2 - f_0 \frac{d\bar{\theta}_{55}}{df_0}}{2 | \bar{\Gamma}_{35} |^2 (1 + \cos \bar{\theta}_0)}. \tag{139}$$

Comparing this equation with (70), we conclude that the band rejected by the band-rejection filter has half the width of the band dropped by a channel-dropping filter using the same rejection cavity. This coincides with the final remark of Section VI. The formulas that yield the dimensions of the rejecting cavity in Section VII can be used, replacing $\bar{Q}_L$ by $\bar{Q}_L/2$.

IX. INTRINSIC Q OF MODE-CONVERSION BAND-REJECTION FILTERS

By definition, the intrinsic Q of a resonating cavity is

$$Q = \omega \left(\frac{\text{energy stored}}{\text{power dissipated as heat}} \right), \tag{140}$$

where ω is the angular frequency.

Let E be the electric field of the resonating mode at any point at the

instant when it passes through a maximum, H the magnetic field at the metallic boundary at the instant when it passes through a maximum, σ the conductivity of the metallic wall, ξ the skin depth and μ and ϵ the permeability and permittivity of free space; then

$$Q = \omega\sigma\xi\epsilon \frac{\int_v E^2 dv}{\int_s H^2 ds}, \tag{141}$$

where v and s are the volume and surface of the waveguide.

For the case of the circular electric filter, the fields inside the cavity are

$$E_{\text{in}} = J_1\left(v_2 \frac{r}{a}\right) \cos \frac{2\pi}{\lambda_{g2}} z, \tag{142}$$

$$H_{\text{in}} = \frac{v_2}{a\omega\mu} J_0(v_2) \cos \frac{2\pi}{\lambda_{g2}} z \tag{143}$$

Outside the cavity, because of the boundary conditions of continuity of the tangential field components, they are

$$E_{\text{out}} \cong J_1\left(v_2 \frac{r}{b}\right) \cos \frac{\pi l}{\lambda_{g2}} e^{-(2\pi/\lambda_{g2\,\text{out}})(|z|-l/2)}, \tag{144}$$

$$H_{\text{out}} \cong \frac{v_2}{b\omega\mu} J_0(v_2) \cos \frac{\pi l}{\lambda_{g2}} e^{-(2\pi/\lambda_{g2\,\text{out}})(|z|-l/2)}. \tag{145}$$

The axial coordinate z has its origin in the center of the cavity; the length of the cavity is l; and

$$\lambda_{g2\,\text{out}} = \frac{\lambda_0}{\sqrt{\left(\frac{v_2\lambda_0}{2\pi b}\right)^2 - 1}}. \tag{146}$$

Substituting (142) through (145) in (141) leads to

$$Q_{\text{TE}_{02}^{\circ}} = \omega\sigma\xi\epsilon \frac{\int_0^b J_1^2\left(v_2 \frac{r}{b}\right) r dr}{\left(\frac{v_2}{a\omega\mu}\right)^2 J_0^2(v_2) a} \cdot \frac{\int_{-l/2}^{l/2} \cos^2 \frac{2\pi z}{\lambda_{g2}} dz + 2\left(\frac{a}{b}\right)^2 \cos^2 \frac{\pi l}{\lambda_{g2}} \int_{l/2}^{\infty} e^{-(4\pi/\lambda_{g2\,\text{out}})(|z|-l/2)} dz}{\int_{-l/2}^{l/2} \cos^2 \frac{2\pi z}{\lambda_{g2}} dz + 2\left(\frac{a}{b}\right) \cos^2 \frac{\pi l}{\lambda_{g2}} \int_{l/2}^{\infty} e^{-(4\pi/\lambda_{g2\,\text{out}})(|z|-l/2)} dz}. \tag{147}$$

Since[13]

$$\int_0^b J_1^2\left(v_2 \frac{r}{b}\right) r dr = \frac{b^2}{2} J_0^2(v_2), \tag{148}$$

$$\frac{a}{b} \cong 1 \tag{149}$$

and

$$\frac{v_2 \lambda_0}{2\pi a} \cong 1, \tag{150}$$

(147) becomes

$$Q_{TE_{02}^\circ} \cong \frac{a}{\xi}, \tag{151}$$

where ξ, the skin depth, is

$$\xi = \sqrt{\frac{2}{\omega\mu\sigma}}. \tag{152}$$

The result (151) coincides with the intrinsic Q of an infinitely long cylindrical cavity resonating with TE_{02}° at cutoff (Ref. 12, p. 59). Similar reasoning for a mode-conversion band-rejection filter in rectangular waveguide yields for the intrinsic Q of the resonating $TE_{20}^\square$ mode:

$$Q_{TE_{20}\square} = \frac{d}{\xi\left(1 + \frac{2d}{a}\right)}, \tag{153}$$

where a and d are the width and height of the rectangular waveguide.

Typical theoretical values in copper waveguides are the following:

For TE_{02}° mode at 5.4 millimeters, $a \cong v_2(5.4/2\pi) = 6.04$ millimeters, and

$$Q_{TE_{02}^\circ} = 21{,}400. \tag{154}$$

This theoretical intrinsic Q is very large compared to the intrinsic Q obtainable in a parallelepiped-shaped cavity. For comparison we calculate the intrinsic Q of a half-wavelength cavity at 5.4 millimeters in the standard RG98U waveguide (0.074 × 0.0148 inches) that we assume to be made out of copper. Using the expression for intrinsic Q given on Ref. 12, p. 55,

$$Q_{TE_{10}\square} = 3460. \tag{155}$$

For $TE_{20}^{\square}$ mode, assuming $a \cong \lambda_0 = 1.2$ inches and $d = 0.4$ inches, expression (153) yields

$$Q_{TE_{20}\square} = 9000. \tag{156}$$

The intrinsic Q of a half-wavelength resonator in RG52U waveguide (0.4×0.9 inch) that we assume made of copper is

$$Q_{TE_{10}\square} = 7990. \tag{157}$$

X. EXPERIMENTAL RESULTS FOR CHANNEL-DROPPING FILTER FROM TE_{01}° TO $TE_{10}^{\square}$

We shall go first through the detailed design procedure of a channel-dropping filter for which the bandwidth is relatively large in order to show the limiting possibilities of these mode conversion filters; the experimental results are quoted later.

The selected center frequency and bandwidth of the dropped channel are 55.5 kmc, ($\lambda_0 = 5.4$ millimeters) and 500 mc. The loaded Q is therefore

$$Q_L = 110. \tag{158}$$

To dimension the filter roughly, we use (105) through (110). We shall use primes to distinguish the approximate sizes from those that are final. From (110), adopting $s = 0$,

$$\delta' \cong 0.1$$

and from (105) through (108), adopting $p = 3$, we find

$$a' = 0.249 \text{ inch},$$

$$b' = 0.226 \text{ inch},$$

$$l_B' = l_R' = 0.168 \text{ inch},$$

$$l' = 0.204 \text{ inch}.$$

If the branching rectangular waveguide is RG98U, $W = 0.148$ inch, $d = 0.074$ inch and the diameter of the coupling hole to the branching arm results, from (109)

$$2c = 0.105 \text{ inch}.$$

Since this value is bigger than the 0.074-inch height of the rectangular guide, a round coupling hole can not provide enough coupling. There are many ways to increase the coupling. One is to build the rectangular

waveguide with its axis not perpendicular to the axis of the round waveguide but parallel to it, providing the coupling through a hole in the narrow wall. One of the ends of the rectangular waveguide must be short-circuited at an odd number of quarters of guide wavelength from the center of the coupling hole. For a fixed size of the hole, the amount of coupling can be increased by decreasing the width of the waveguide W, because the waveguide gets closer to cutoff. Another solution consists in wrapping around the $TE_{02}°$ cavity a rectangular waveguide and providing the necessary mode selective coupling between them by means of several holes. The details are given in Ref. 2.

The obvious third solution, and the one we adopt, is to increase the size of the coupling hole to the total cross section of the rectangular waveguide. If the coupling is too large, it can be decreased by displacing the hole to one side of the cavity.

The strong perturbation of the field in the branching cavity due to such a large coupling hole modifies the scattering coefficients calculated in previous paragraphs, and the final length of this cavity, as well as the distance to the rejecting one, must be selected experimentally. The discrepancy between theoretical and experimental values is not large.

10.1 *Design of the Rejecting Cavity*

The design of the rejecting cavity requires the simultaneous solution of (80) and (83) for the determination of the three quantities a, b and l_R. Thus, one of those quantities can be selected arbitrarily.

A good criterion for this selection consists in demanding that at midband frequency the cutoff radius for $TE_{02}°$ is

$$\frac{v_2\lambda_0}{2\pi} = \frac{a+b}{2} = a\left(1 - \frac{\delta}{2}\right) \tag{159}$$

because with this selection midband is equally separated from the two extreme frequencies that limit the proper operation of the filter. These are a lower frequency that cuts off the $TE_{02}°$ in the large waveguide, invalidating the inequality (67), and an upper one that cuts off $TE_{02}°$ in the smaller waveguide and above which propagation of $TE_{02}°$ in that waveguide starts.

Incidentally, it is interesting to notice that, for the frequency $f = f_0 + \Delta f$,

$$\left(\frac{\lambda_0'}{\lambda_{g2}'}\right)^2 = \left\{1 - \left[\frac{v_2\lambda_0}{2\pi a\left(1 + \frac{\Delta f}{f_0}\right)}\right]^2\right\}\left(1 + \frac{2\Delta f}{f_0}\right) \tag{160}$$

becomes, through the use of (159),

$$\left(\frac{\lambda_0'}{\lambda_{g2}'}\right)^2 = 2\left(\delta + \frac{\Delta f}{f_0}\right), \tag{161}$$

and the inequality (67) can be written

$$\frac{\Delta f}{f_0} \ll \delta. \tag{162}$$

This implies that the approximations hold as long as the relative frequency departure from midband is small compared to the relative diameter change.

Another criterion for the selection of a, b or l_R may arise from the advantage of using standard-size waveguides already available, as long as the limiting frequencies discussed previously are not approached. Following this procedure for a standard laboratory waveguide with

$$2a = \tfrac{7}{16} \text{ inch}, \tag{163}$$

the simultaneous solution of (80) and (83) yields

$$2b = 0.5 \text{ inch and} \tag{164}$$

$$l_R = 0.234 \text{ inch}. \tag{165}$$

The measured performance of this band-rejection filter is shown in Fig. 13. The agreement between theoretical and experimental values is excellent.

10.2 *Design of the Branching Cavity*

Ignoring the effect of the coupling hole between the branching waveguide and cavity, the dimensions should be those of the rejecting cavity given in (163), (164) and (165).

The distance between centers of the resonating cavities, according to (82) with $p = 4$, should be

$$l_d = 0.572 \text{ inch}.$$

The number of quarters of wavelength between centers of cavities is nine. Experimentally it was found impossible to reduce l_d because the $TE_{02}°$ mode, being close to cutoff in the small waveguide, couples to the other cavity. The final dimensions, as well as the performance of the assembled channel-dropping filter, are shown in Fig. 14.

The relatively high insertion loss for the dropped channel cannot be

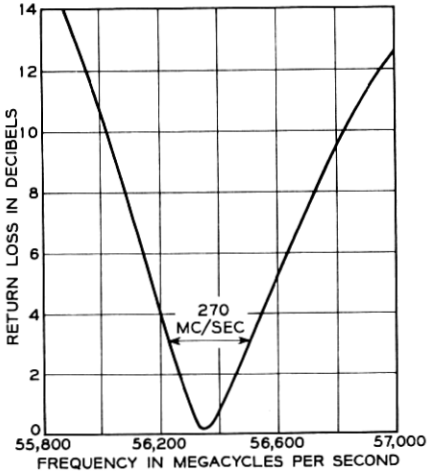

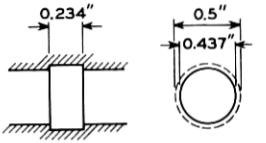

	THEORETICAL	EXPERIMENTAL
MIDBAND	55.5 KMC/SEC	56.35 KMC/SEC
LOADED Q	222	209
INTRINSIC Q	21,400	11,800

Fig. 13 — Performance of circular-electric band-rejection filter.

accounted for by heat losses because of the good performance of the band-rejection filter. Thus, mode conversion due to the asymmetry of the coupling to the rectangular waveguide must be its cause. Loss should be reduced using distributed coupling to the rectangular waveguide, as in Ref. 2.

Pictures of the filter are shown in Figs. 15 and 16.

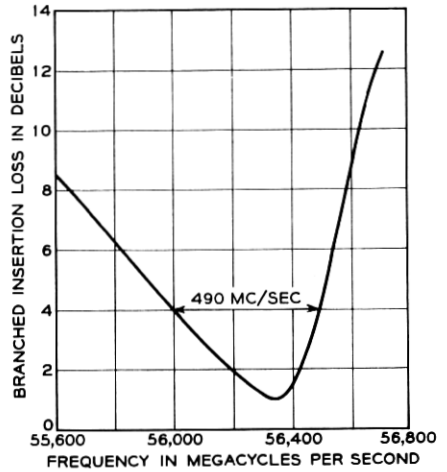

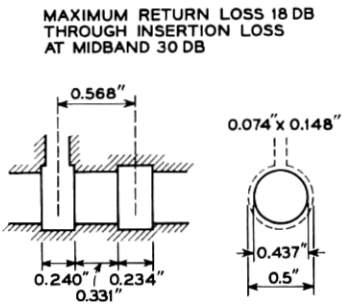

	THEORETICAL	EXPERIMENTAL
MIDBAND	55.5 KMC/SEC	56.35 KMC/SEC
LOADED Q	111	115

Fig. 14 — Performance of mode-conversion channel-dropping filter.

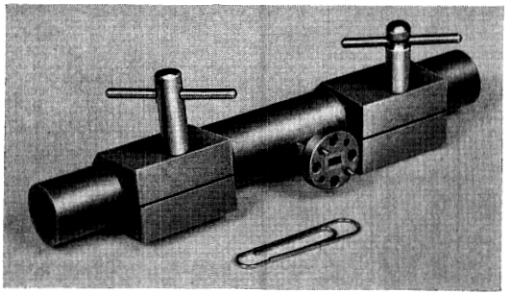

Fig. 15 — Mode-conversion channel-dropping filter.

10.3 *Band Rejection Filters in Different Waveguides*

Figs. 17, 18 and 19 show the geometry and experimental results for different band-rejection filters in round and rectangular waveguide. Those filters that have constant metallic cross section have generation and resonance of a higher-order mode in the region where the dielectric is located. For the case of Fig. 19, it has been shown in Ref. 11 that a rectangular waveguide with a dielectric slab is equivalent to a rectangular waveguide that has a width increase for a length equal to that of the slab. Calling d the width of the slab, ζ the distance to the near narrow wall and ϵ_d the permittivity of the dielectric, the relative apparent in-

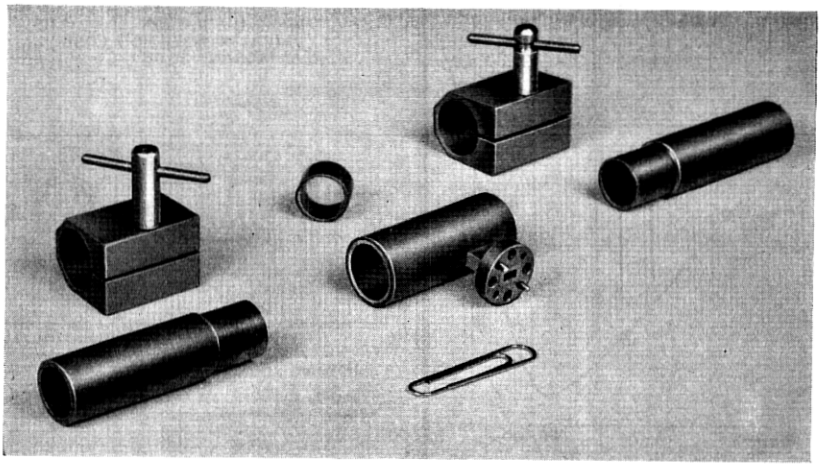

Fig. 16 — Exploded view of mode-conversion channel-dropping filter.

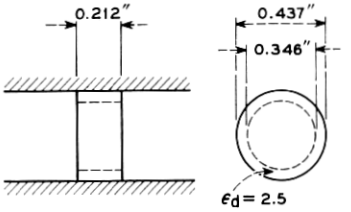

MIDBAND	56.45 KMC/SEC
LOADED Q	213
INTRINSIC Q	2000
RETURN LOSS AT MIDBAND	1 DB

Fig. 17 — Band-rejection filter of TE_{01}° mode (polystyrene ring; $\epsilon_d = 2.5$).

crease of the waveguide width is

$$\delta = \frac{4\pi^2}{3}\frac{d^3}{a\lambda_0^2}\left(\frac{\epsilon_d}{\epsilon} - 1\right)\left[1 + \frac{3\zeta(\zeta + d)}{d^2}\right].$$

With this value known, all the design formulas in Section VII can be used.

In the round waveguide in which only circular-electric modes are of interest, tuning is available by changing the physical length of the resonating cavity. For that purpose a telescopic type of junction is ideal,

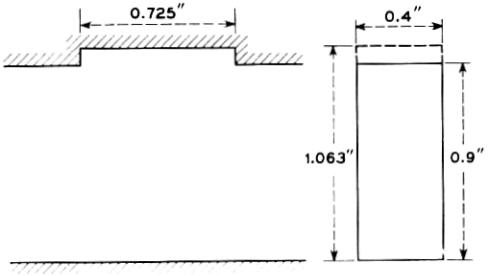

MIDBAND	12.3 KMC/SEC
LOADED Q	92
INTRINSIC Q	3500
RETURN LOSS AT MIDBAND	~0.2

Fig. 18 — Band-rejection filter of TE_{10}□ mode.

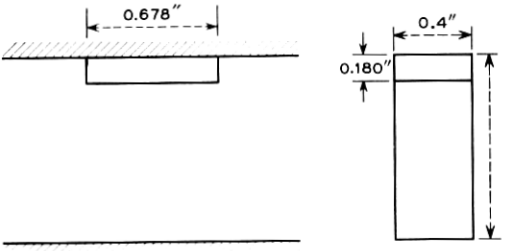

MIDBAND	12.2 KMC/SEC
LOADED Q	66
INTRINSIC Q	2280
RETURN LOSS AT MIDBAND	~0.2 DB

Fig. 19 — Band-rejection filter of TE_{10}□ mode (polystyrene ring; $\epsilon_d = 2.5$).

since the cracks do not interrupt the conduction current and since it is very easy to manufacture. One tube of inner diameter $2a$, inside of which two tubes of outer diameter $2a$ and inner diameter $2b$ can slide, will suffice.

The tuning in the case of Fig. 17 can be achieved by trimming the dielectric. For the filters in rectangular waveguide, Figs. 18 and 19, one tuning screw at each one of the electric-field maxima of the resonating mode provide the tuning.

XI. CONCLUSIONS

Resonance of higher-order modes in waveguides has been advantageously used to make very simple band-rejection filters of unusually low loss. In particular, the filter operating with circular-electric modes has an intrinsic Q that is one order of magnitude better than the intrinsic Q of conventional (cavity or lumped) band-rejection filters operating at the same frequency.

Mode-conversion band-rejection filters have been used as building blocks for the construction of channel-dropping filters that simultaneously produce the band separation and the transfer from $TE_{01}{}^{\circ}$ mode to $TE_{10}{}^{\square}$ required in the long distance waveguide communication system.[1] One model operating at 56.3 kmc has a bandwidth of 490 mc, and the insertion loss for the dropped channel is 1 db.

Although the emphasis in this paper has been on filters operating mainly with circular-electric modes in round waveguides and TE modes in rectangular waveguides, the calculations are quite general and can be applied in any scheme in which mode-conversion filters are used.

XII. ACKNOWLEDGMENT

The author is indebted to D. L. Bisbee for performing the measurements.

XIII. LIST OF SYMBOLS

a = radius of the resonant cylindrical cavity or width of the resonant rectangular waveguide.

b = radius of the through cylindrical waveguide or width of the through rectangular waveguide.

c = radius of the coupling hole between resonant cavity and branching arm.

d = height of any rectangular waveguide.

f = frequency.

f_0 = midband frequency.
l = distance between cavities.
l_B = length of branching cavity.
l_d = distance between centers of cavities.
l_R = length of rejecting cavity.
$2p + 1$ = number of nonresonant mode quarter-wavelengths between centers of branching and rejecting cavities (p is an arbitrary integer).
$2s + 1$ = number of resonant mode half wavelengths in each cavity (s is an arbitrary integer).
Q = intrinsic Q.
Q_L = loaded Q.
S_{mn} = scattering coefficient of a half cavity or a more complicated circuit.
W = width of the branching rectangular waveguide.
Y = admittance.
Γ_{mn} = scattering coefficient of elementary structures.
δ = relative diameter change or width change of through waveguide.
ϵ = permittivity of free space.
ϵ_d = permittivity of dielectric.
θ = electrical difference between two energy paths.
θ_0 = midband electrical difference between two energy paths.
θ_{mn} = phase of the scattering coefficients of junctions with wave guides reduced to zero length.
λ = midband free-space wavelength.
λ_{g1} = midband guided wavelength of the nonresonant mode.
λ_{g2} = midband guided wavelength of the resonant mode.
μ = permeability.
ν_n = nth root of the J_1 function.
σ = conductivity of metal.
φ_0 = midband electrical length of the resonating cavity in terms of the resonating mode.
ψ = midband electrical distance between cavities in terms of the through mode.
ψ_d = midband electrical distance between centers of cavities in terms of the through mode.
ψ_1 = electrical distance between the branching cavity discontinuities in terms of the non-resonating mode.
ψ_{10} = midband electrical distance between the branching cavity discontinuities in terms of the non-resonating mode.

ψ_2 = electrical distance between the branching cavity discontinuities in terms of the resonating mode.

ψ_{20} = midband electrical distance between the branching cavity discontinuities in terms of the resonating mode.

$\bar{\psi}_1$ = electrical distance between the rejecting cavity discontinuities in terms of the nonresonating mode.

$\bar{\psi}_{10}$ = midband electrical distance between the rejecting cavity discontinuities in terms of the nonresonating mode.

$\bar{\psi}_2$ = electrical distance between the rejecting cavity discontinuities in terms of the resonating mode.

$\bar{\psi}_{20}$ = midband electrical distance between the rejecting cavity discontinuities in terms of the resonating mode.

REFERENCES

1. Miller, S. E., Waveguide as a Communication Medium, B.S.T.J., **33,** 1954, p. 1209.
2. Marcatili, E. A., Channel-Dropping Filter in the Millimeter Region Using Circular-Electric Modes, to be published.
3. Marcatili, E. A., A Circular-Electric Hybrid Junction and Some Channel-Dropping Filters, this issue, p. 185.
4. King, A. P. and Marcatili, E. A., Transmission Loss Due to Resonance of Loosely Coupled Modes in Multi-Mode Systems, B.S.T.J., **35,** 1956, p. 899.
5. Marcatili, E. A., Mode Conversion Filters, I.R.E. Wescon Conv. Rec., 1958, part 1.
6. Jaynes, E. T., Ghost Modes in Imperfect Waveguides, Proc. I.R.E., **46,** 1958, p. 416.
7. Vogelman, J. H. Microwave Rejection Filters Using Higher-Order Modes, I.R.E. Trans., **MTT-7,** 1959, p. 461.
8. Goubau, G., *Electromagnetische Wellenleiter und Hohlraume*, Wissenschaftliche Verlagsgesellschaft, Stuttgart, Germany, 1955.
9. Marcuvitz, N., ed., *Waveguide Handbook*, M.I.T. Radiation Laboratory Series, Vol. 10, 1st ed., McGraw-Hill, New York, 1951, p. 108.
10. Bethe, H. A., Theory of Diffraction by Small Holes, Phys. Rev., **66,** 1944, p. 163.
11. Marcatili, E. A., Scattering at a Sudden Change of Cross Section in Multimode Waveguide, to be published.
12. Montgomery, C. G., Dicke, R. H. and Purcell, E. M., eds., M.I.T. Radiation Laboratory Series, Vol. 8, 1st ed., McGraw-Hill, New York, 1948.
13. McLachlan, N. W., *Bessel Functions for Engineers*, Clarendon Press, Oxford, 1934.